

Design and Experimental Optimization of a Canister Antenna for 18-GHz Operation

C. A. SILLER, JR., P. E. BUTZIEN, and
J. E. RICHARD

(Manuscript received May 27, 1977)

The design and experimental optimization of a canister antenna for operation in the 17.7 to 19.7 GHz frequency band are described. The canister is specifically designed to accommodate the antenna, transmitter and receiver units, and to be aesthetically innocuous in its environment. The basic antenna configuration, that of a shielded inverted periscope, is reviewed. Details of the constituent parts of the antenna, including dual mode feed, paraboloidal reflector, mirror, radome, and microwave absorber are presented. The influence that each of these items plays in determining net electrical performance is identified, including (where appropriate) steps taken to achieve electrical optimization. The antenna is shown to afford excellent sidelobe suppression, azimuthal plane cross polarization discrimination in the mid to upper 30 dB range, and a return loss of better than 23 dB. The gain efficiency is approximately 62 percent and is essentially polarization independent.

I. INTRODUCTION

The design and experimental optimization of a canister antenna for point-to-point operation in the 17.7 to 19.7 GHz frequency band are described in this paper. The antenna, which has been briefly described earlier,¹ was designed for a digital radio system (DR 18A).² The system will use a 274-Mb/s quaternary phase shift keying (QPSK) modulation to provide eight radio channels (seven working, one protection). Each channel provides 4032 voice circuits. Anticipated typical repeater spacings will be 2.4 to 7.2 kilometers.³ The canister is specifically designed to accommodate the antenna, transmitter and receiver units, and to be aesthetically innocuous in its environment.

The initial antenna concept was first proposed by Crawford and Turrin⁴ in 1969. Subsequently, the authors, drawing in part upon the-



Fig. 1—DR 18A repeater site located in Methuen, Massachusetts.

oretical and experimental work of colleagues at Bell Laboratories, designed an antenna for incorporation into a mast-supported, integrated canister antenna concept. A photograph of an existing repeater site in Methuen, Massachusetts, which may be characterized as "typical" in appearance, is presented in Fig. 1.

As depicted in the cut-away view in Fig. 2, the antenna is basically a shielded inverted periscope consisting of a paraboloidal reflector, feed assembly, mirror and inclined radome. The feed, the end of which is located at the focal point of the parabolic dish, illuminates the paraboloid with a spherical wave. Upon reflection, the energy is converted to a plane

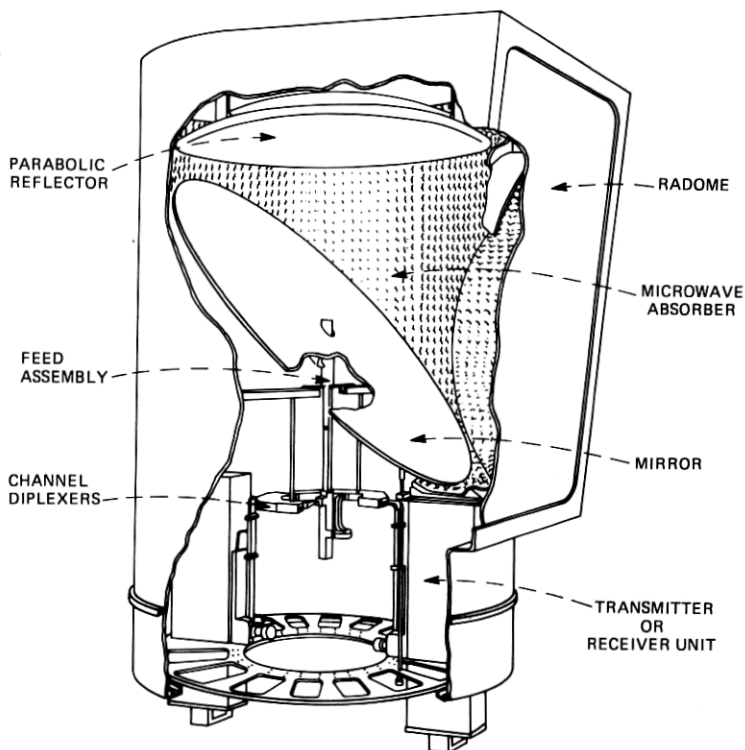


Fig. 2—Schematic depiction of canister antenna showing salient features.

wave which is subsequently incident upon a mirror nominally inclined at 45° to the paraboloidal axis. The energy is then reflected from the mirror (which is tiltable to deflect the beam up or down slightly) and exits through the circular aperture. Low wide-angle sidelobes are achieved by relying upon the absorber-lined canister to afford electromagnetic shielding and reduce edge diffraction at the aperture. It may also be noted from this figure that the canister serves as housing for the microwave networks as well as transmitter and receiver modules. This paper deals specifically with the influence of the various components of the antenna on its electrical performance and (where appropriate) steps taken to achieve electrical optimization.

Electrical objectives to be attained in the antenna design are dictated by the radio system. After a study into the regional variation of rainfall and its role in setting repeater spacings, the gain objective was established as approximately 42 dB above isotropic at the low edge of the frequency band since gain increases with frequency. This gain objective included transmission loss through the radome. The radiation pattern determines the maximum number of radio paths which may converge

at a point. With a goal of eight such paths and a desired discrimination of 60 dB, the pattern was to drop to ≤ -60 dB at 45° in azimuth. Finally, the return loss of the dish and window was to exceed 26 dB, i.e., voltage reflection ≤ 0.050 .

Considerations involved in the selection of a suitable feed are reviewed. Since the influence of the feed pattern on gain cannot be divorced from the selection of a paraboloid, the inter-relationship of feed taper and dish f/D ratio is delineated by computing both illumination and spillover efficiencies to obtain net antenna efficiency. The optimum position of the feed with respect to the mirror is also explored, and the influence of the hole around the feed on antenna radiation patterns is elucidated. The wide-angle radiation suppression of the antenna is shown to be acutely dependent upon the use of broadband microwave absorber. Since antenna directivity is also affected by the presence of a radome, the tilt of the mirror, and the correct positioning of the feed, the role which these items play in influencing radiation suppression is assessed. Measured return loss and the sources which give rise to reflected power are also discussed. The paper is concluded with a summary of the electrical characteristics of the antenna design.

II. ANTENNA FEED

2.1 Properties of dual mode feeds

An objective in the design of this antenna was the attainment of circularly symmetric feed patterns for the illumination of the paraboloid. It may readily be shown that such a feed, with an illumination function characterized by

$$E_\theta = AF(\theta) \sin \phi \quad (1)$$

$$E_\phi = AF(\theta) \cos \phi \quad (2)$$

$$|E| = (E_\theta^2 + E_\phi^2)^{1/2} = AF(\theta) \quad (3)$$

where θ, ϕ are the conventional spherical coordinates, results in a completely linearly polarized field distribution after reflection from a full paraboloid. As a consequence, there are no cross polarized fields in the aperture. In addition, this feed illumination readily permits one to design for optimum polarization-independent gain.

Fields like those given in eqs. (1) and (2) are achieved by using dual mode and hybrid mode feeds. For this antenna, a dual mode feed was found to be effective, as well as simpler and less costly to produce than the hybrid mode feed. Chu⁵ has noted that the observed radiation pattern of a dual mode feed is approximated closely by the H-plane pattern of an open-ended circular waveguide excited by the dominant TE_{11}^0 mode:

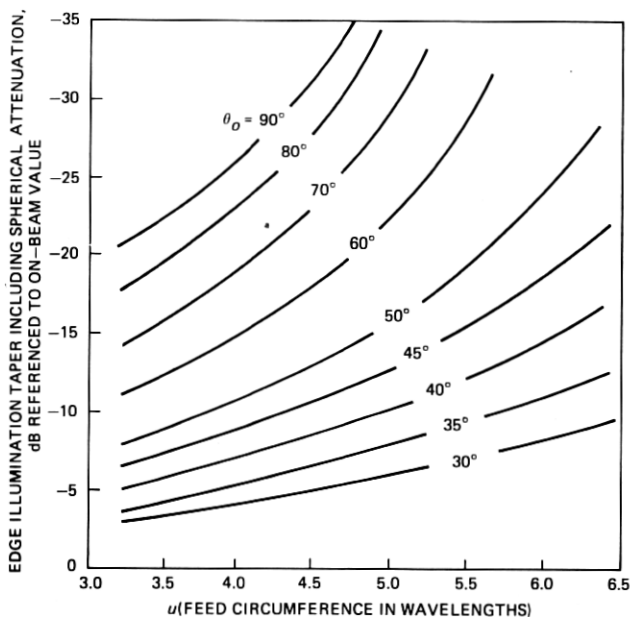


Fig. 3—Characterization of feed illumination, including spherical attenuation to a paraboloidal surface, for various values of the subtended dish half-angle, θ_0 .

$$F(\theta) = [\sqrt{1 - (1.841/u)^2} + \cos \theta] \cdot \frac{J_1(u \sin \theta)}{1 - \left[\frac{u \sin \theta}{1.841} \right]^2} \quad (4)$$

where $u = \pi d/\lambda$, d is the diameter of the feed waveguide, λ is the wavelength of the applied signal, and θ is the angle measured from the axis of the feed. The region of validity for eq. (4) is $\pi \leq u \leq 2\pi$, or equivalently, the waveguide diameter is limited to one to two wavelengths.

The field intensity at the edge of a paraboloidal reflector may be computed as a function of u by using eqs. (3) and (4) and including spherical attenuation to the paraboloidal surface, $\cos^2(\theta/2)$. The latter comes from the fact that the equation of a paraboloid in spherical coordinates is $r = 2f/(1 + \cos \theta)$. The results of such a computation are presented in Fig. 3 for various values of θ_0 , the subtended half-angle of the paraboloid. The use of θ_0 instead of f/D is preferred by the authors because of its simpler physical interpretation. It is noted that $f/D = 1/(4 \tan \theta_0/2)$, where f and D are the focal length and reflector diameter, respectively. From Fig. 3, selection of any two of the following three variables uniquely specifies the third: edge taper in decibels, feed diameter in wavelengths, and subtended half-angle in degrees. The utility of this figure arises in optimizing the gain efficiency of the antenna, the subject of the next section.

2.2 Relationship of feed taper to efficiency

The gain efficiency of a center-fed full paraboloid may be broken down into an illumination efficiency and spillover efficiency (as in Ref. 6). The concept of an illumination efficiency is well known; spillover efficiency specifies that fraction of the total power radiated by the feed which is intercepted by the paraboloidal dish. Denoting these terms by η_i and η_s , respectively, they are mathematically evaluated from the feed illumination function. Namely,

$$\eta_i = \frac{\left| \int_{\phi=0}^{2\pi} \int_{\theta=0}^{\theta_o} F(\theta) \cos^2 \left(\frac{\theta}{2} \right) d\Sigma \right|^2}{A_p \int_{\theta=0}^{2\pi} \int_{\theta=0}^{\theta_o} \left| F(\theta) \cos^2 \left(\frac{\theta}{2} \right) \right|^2 d\Sigma} \quad (5)$$

In eq. (5), the projected aperture area is

$$A_p = 4\pi f^2 \frac{1 - \cos \theta_o}{1 + \cos \theta_o}$$

and the integration is performed over the projected aperture of the reflector with differential area element

$$d\Sigma = \frac{f^2 \sin \theta}{\left(\cos \frac{\theta}{2} \right)^4} d\theta d\phi$$

The spillover efficiency is given by

$$\eta_s = \frac{\int_0^{\theta_o} [F(\theta)]^2 \sin \theta d\theta}{\int_0^{\pi/2} [F(\theta)]^2 \sin \theta d\theta} \quad (6)$$

The total antenna gain efficiency is expressed by the product, viz. $\eta_a = \eta_i \eta_s$. The evaluation of η_s given by eq. (6) is approximate insofar as it neglects back radiation from the feed. Radiation into the hemisphere $\pi/2 \leq \theta \leq \pi$, $0 \leq \phi \leq 2\pi$ is not accurately described by eq. (4), and is so low as to contribute virtually nothing to the evaluation of η_s .

The terms η_a and η_s have been computed as a function of dish edge illumination (spherical attenuation and feed taper at an angle θ_o) for a variety of subtended half-angles. (Selection of a dish edge illumination and half-angle implicitly determines a feed diameter as shown in Fig. 3). Typical aperture efficiencies, expressed in decibels down from full area gain, are presented in Fig. 4. The figure shows that for a specified angle θ_o , the optimum efficiency occurs for edge tapers of -11.5 to -12.5

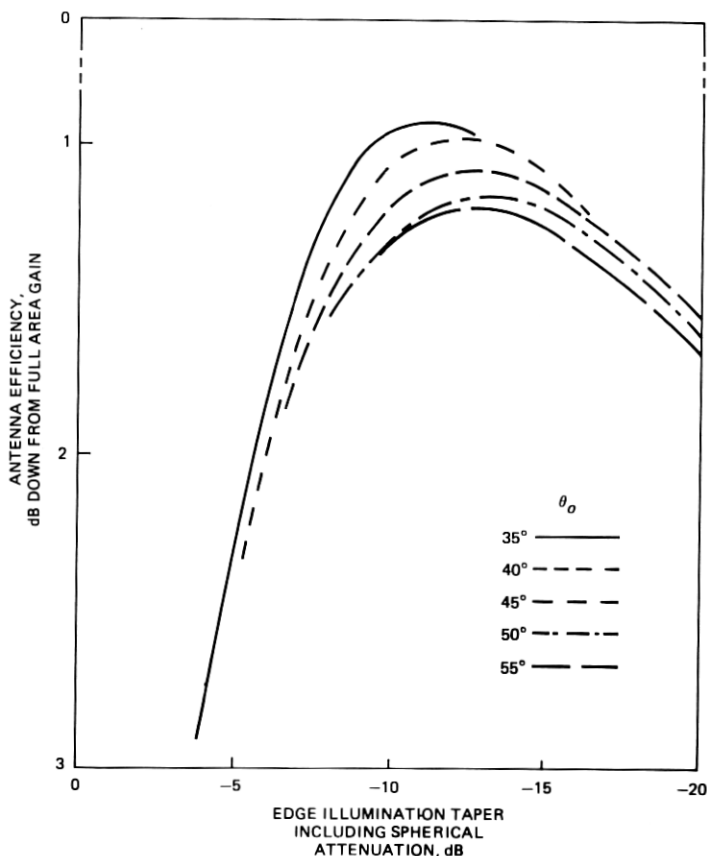


Fig. 4—Antenna efficiency as a function of edge illumination for various values of subtended dish half-angle, θ_0 .

dB. Additionally, for optimum taper, the least loss in gain occurs for a half-angle of approximately 35°.

While it would appear from the above analysis that a half-angle of 35° should be selected, two additional considerations are germane. First, from an electrical standpoint, edge tapers of -11.5 to -12.5 dB for small values of θ_0 necessitate relatively large feed diameters (See Fig. 3). Large feed diameters are deleterious because they can support higher order modes, the effect of which will be demonstrated subsequently. They also increase feed blockage in the antenna, thus deteriorating sidelobe suppression in the radiation pattern. In regard to this latter point, theoretical analyses of this antenna by Anderson⁷ indicate that the sidelobe levels in that angular region where the imaged paraboloid would be visible to an observer are insensitive to field illumination at the edge of the dish, an observation that has been experimentally substantiated elsewhere.

within Bell Laboratories. He concluded that the level of radiation suppression is principally influenced by feed blockage. This conclusion is validated by an experimental study discussed later in the paper. The second point arguing against a 35° half-angle is aesthetic, in that such a paraboloid would require a canister more slender and tall than considered appropriate. Feed blockage is estimated to have a negligible effect on the gain of this antenna.

There is also a reason why angles greater than 45° are not especially desirable. The geometry of the antenna dictates that for angles greater than 45° , the feed must protrude above the mirror. Yet experimental evidence indicates that this, too, manifests itself as feed blockage, and can deteriorate sidelobe suppression. For these reasons, a subtended half-angle of 40° appeared reasonable.

As stated in the Introduction, the gain objective of this antenna was approximately 42 dBi at 17.7 GHz. Experience indicates that it is difficult to realize gain within 0.5 dB of theoretical, so the antenna was designed to theoretically provide a gain of 42.5 dBi. Using Fig. 4 with $\theta_o = 40^\circ$ implies that this gain is achieved by selecting a reflector diameter of 0.813 meters and $f = 0.559$ meters. Because of limitations in available tools for spinning the dish, a focal length of 0.536 meters was actually used. For a dish of 0.813-meter diameter, this corresponds to $\theta_o = 41.4^\circ$ or $f/D = 0.66$. Tolerances of the spun aluminum paraboloid were 0.0254 centimeters rms and a peak deviation of less than 0.0305 centimeters from the design surface. At 19.7 GHz, the highest anticipated operating frequency, these correspond to $\lambda/60$ and $\lambda/50$, respectively.

2.3 Feed designs and performance

Two dual mode configurations (as depicted in Fig. 5) of square and circular cross section with a variety of aperture sizes were considered. The principle of operation of these dual mode configurations is that of achieving a two-mode mixture of fields at the feed aperture such that the edge currents are nearly zero.⁸ In Fig. 5, we may consider a TE_{11}^o mode (for the case of circular cross section) propagating upward from the uniform waveguide at plane a . This wave encounters an abrupt change in cross section at plane b such that the electric field is bent to maintain a vanishing tangential component at the conducting walls. An axial component of the total electric field (E_z) is thereby generated and by plane c conversion of some of the energy to the TM_{11}^o mode has been accomplished. The distance from c to d provides the proper phasing of the two modes at the feed aperture since the two modes propagate at different phase velocities. Since the two modes do travel with different phase velocities, the feed does have a bandwidth limitation. Nevertheless, the feed provides proper performance across the 17.7 to 19.7 GHz band.

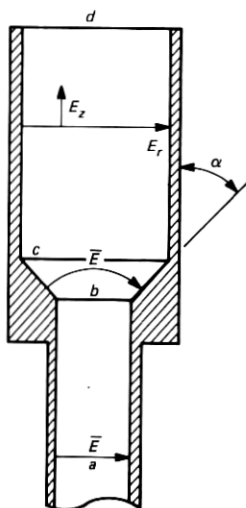


Fig. 5—Dual mode feed cross section.

Two sizes of dual mode feed were built and tested in both the round and square cross section geometries. The feeds of square cross section were found to have higher cross polarized fields in the $\pm 45^\circ$ planes than the circular feeds, and were therefore no longer considered.

Two sizes of feed were built because the aperture diameter-to-wavelength ratio determines the illumination taper of the feed. As noted above, the canister antenna was designed with a subtended half-angle of approximately 41.4° between the feed and rim of the paraboloid. To attain optimum gain efficiency for this $0.66\text{-}f/D$ paraboloid fed by a dual mode feed requires an edge illumination (including spherical attenuation to the paraboloidal surface of just over 1.1 dB at 41.4°) of -12.1 dB (from Fig. 4). Using Fig. 3, such a feed requires $u = 5.4$ and hence has a diameter of 2.92 centimeters at 17.7 GHz. This diameter, however, allows four higher-order modes to propagate between planes c and d (Fig. 5). Therefore, a smaller version with a 2.44-centimeter diameter which just cuts off beyond the TM_{11}^0 mode was also built. Both of these models had cone angles of $\alpha = 30^\circ$.

It was found that due to higher order modes (TM_{21}^0 , TE_{41}^0 , TE_{12}^0 , and TM_{02}^0) which could propagate, the larger diameter feed produced H-plane radiation patterns which fell off much too rapidly over a large part of the frequency range of interest. This effect is depicted in Fig. 6a.

The 2.44-centimeter diameter dual mode feed was extensively tested and was subsequently chosen as the feed for this antenna. The length of the drift section was adjusted empirically to 3.81 centimeters to obtain the best match of E-plane and H-plane taper at mid-band. The feed il-

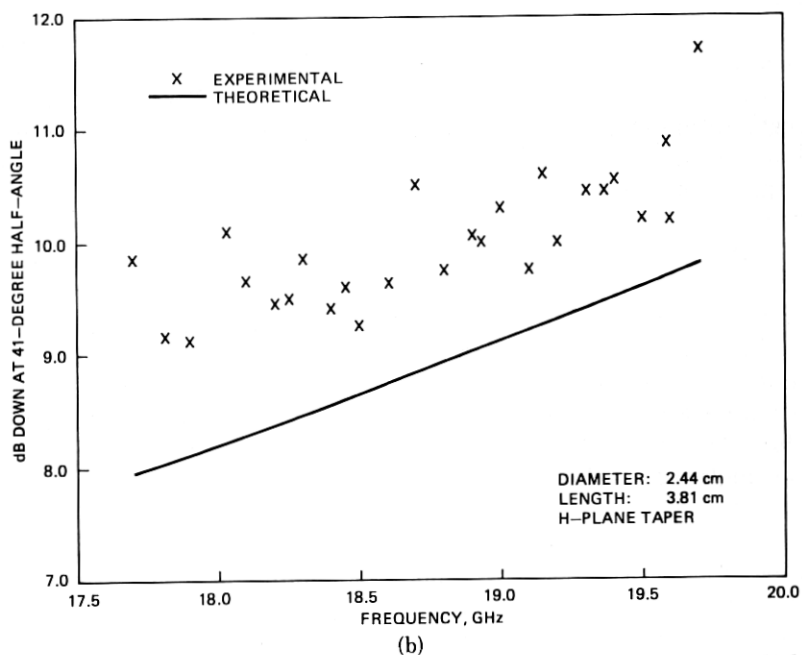
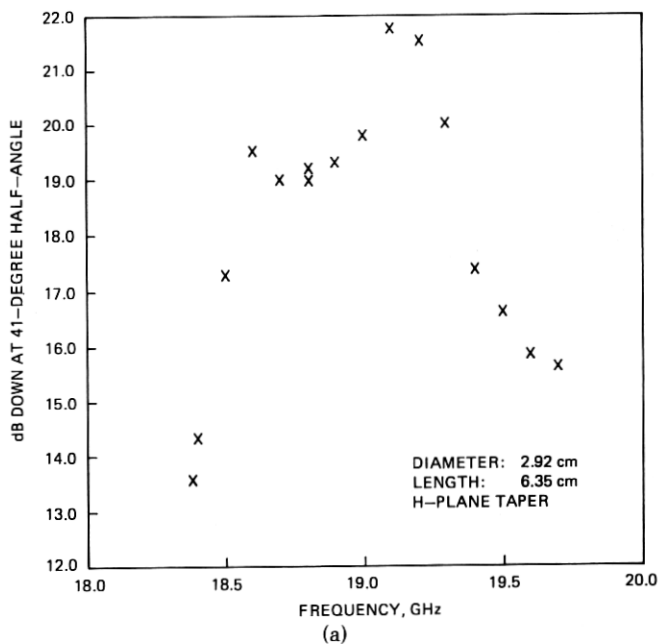
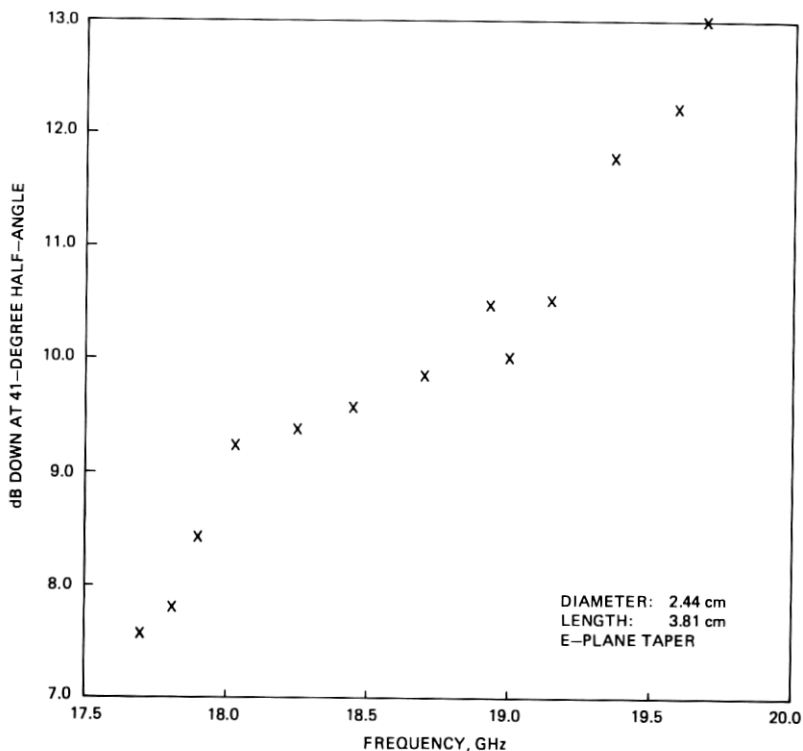


Fig. 6—Dual mode feed tapers as a function of frequency: (a) H-plane measured edge tapers of a 2.92-centimeter diameter dual mode feed; (b) H-plane measured and theoretical edge tapers of a 2.44-centimeter diameter dual mode feed; (c) E-plane measured edge tapers of the 2.44-centimeter diameter dual mode feed.



(c)
Fig. 6 (continued)

lumination tapers (no spherical attenuation) as a function of frequency for the H-plane and E-plane are shown in Figs. 6b and 6c, respectively.* Each point represents the power average of the edge taper at 41° on both sides of the feed radiation pattern like those shown for the E- and H-planes at 17.7 GHz, 18.7 GHz, and 19.7 GHz in Figs. 7a, 7b, and 7c, respectively. The patterns in Figs. 7a, 7b and 7c were measured on a small indoor range. Note from Figures 6b and 6c that E-plane and H-plane tapers are the same only near the design frequency, implying best illumination symmetry at that point. As the signal frequency departs from the design frequency, the illumination in the aperture of the paraboloid becomes increasingly asymmetric, an assessment of which may be obtained from these figures. For example, note from Figures 6b, 6c, and 7a that at 17.7 GHz, the H-plane taper at the edge of the dish is measured to be approximately -9.8 dB, while at this same frequency the E-plane

* As Figs. 6b and 6c show, the final antenna feed was tested at more frequencies in the H-plane than in the E-plane. This was done to assure that difficulties which were manifest in the over-moded feed (see Fig. 6a) did not occur in the smaller feed.

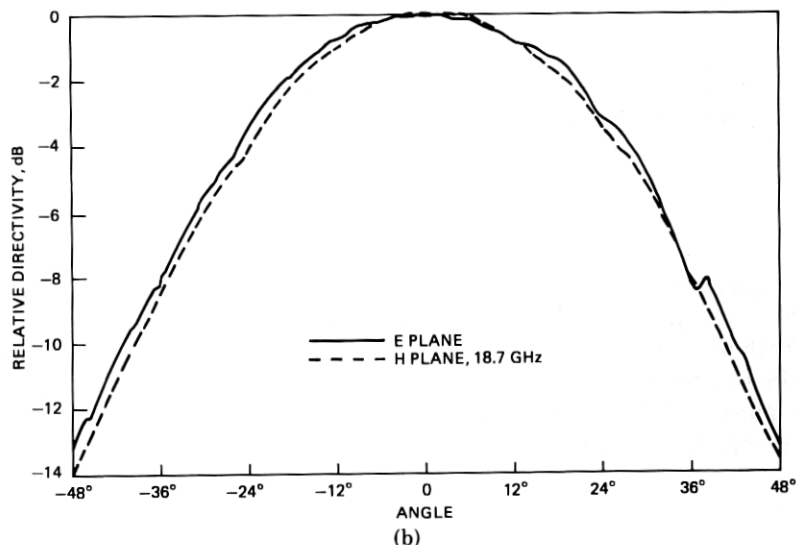
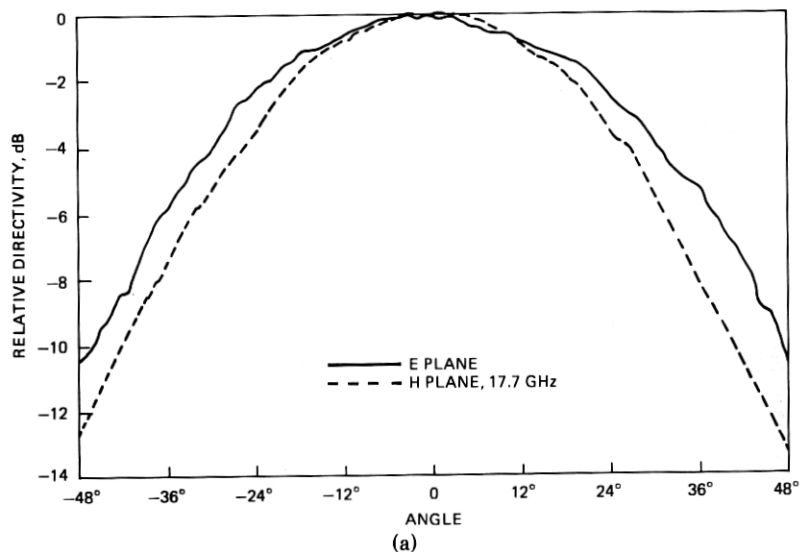


Fig. 7—E- and H-plane radiation patterns of the 2.44-centimeter diameter dual mode feed: (a) 17.7 GHz; (b) 18.7 GHz; (c) 19.7 GHz.

taper is approximately -7.6 dB. Figure 6b also contains theoretical H-plane tapers computed from eq. (4). As the data reveals, at 41° measured tapers exceed the theoretical values by approximately 1 dB. This observation is also valid for other dual mode feeds with which the authors are familiar. Note that the measured taper at 18.7 GHz is very close to the optimum (see Fig. 4).

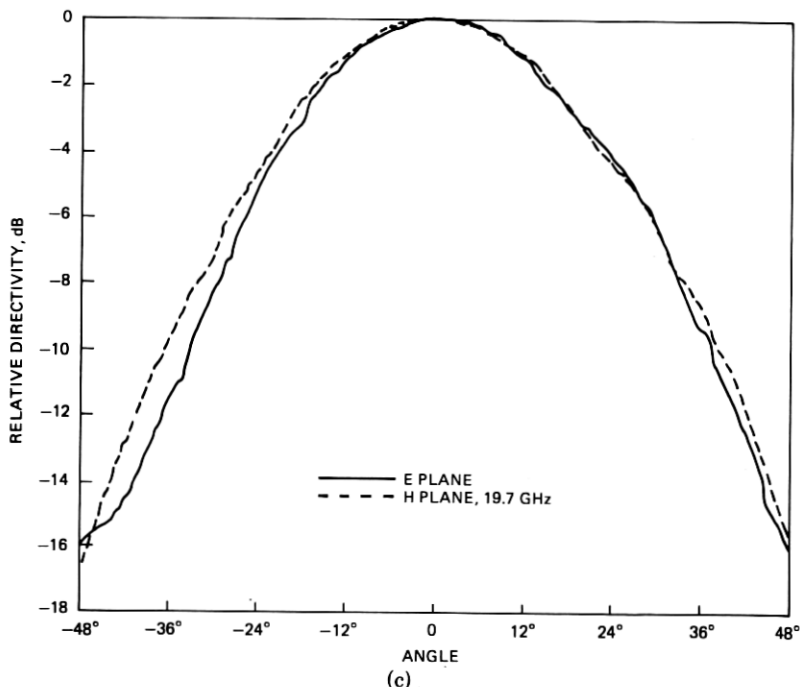


Fig. 7 (continued)

Cross polarized patterns were also measured in both the E and H principal planes and the $\pm 45^\circ$ planes. The patterns were generally room-reflection limited to better than a 40-dB dynamic range, thereby inferring the capability of measuring cross polarized fields to that level. Measurements made at more than ten frequencies within the 17.7 to 19.7-GHz band indicate that near boresight the cross polarized response approaches the upper 30 dB range in the $\pm 45^\circ$ planes. Because the antenna is circularly symmetric from a geometrical optics viewpoint, the reflector system itself adds little to cross polarization conversion except for small contributions from surface roughness and feed scattering. The antenna polarization properties are essentially set by the feed itself.

The theoretical gain efficiency of the antenna has been calculated for 41.4° and is plotted in Fig. 8 as a function of field taper at the rim of the paraboloid. Also indicated on this curve is the taper achieved with the 2.44-centimeter diameter feed at 17.7 GHz, 18.7 GHz, and 19.7 GHz (obtained from a robust linear regression of data in Figs. 6b and 6c). As this figure indicates, the feed should afford near optimum performance since the highest efficiency is predicted for the upper portion of the band where rain attenuation can be expected to be most severe.

The gain of this antenna without the radome was measured on an

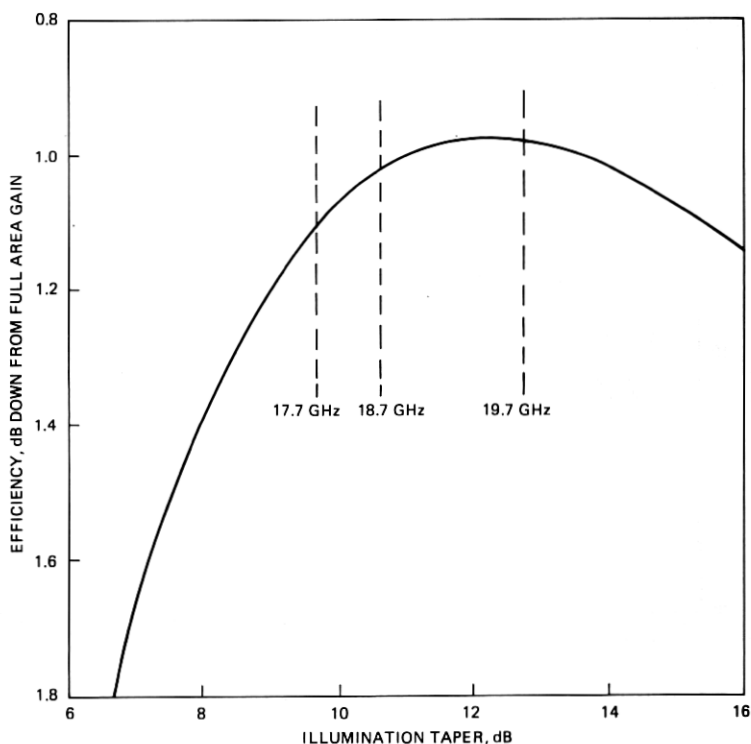


Fig. 8—Theoretical efficiency of prototype design as a function of illumination taper at edge of dish.

outdoor range using the comparison method and a standard gain horn as a reference calibration. The measured gain, relative to an isotropic radiator, and aperture efficiency are stated in Table I. Observe that higher gain for the upper portion of the frequency band has been achieved.

Experience obtained during an earlier CW experiment using this antenna concept has indicated the necessity to avoid insects and other foreign matter getting into the feed and altering electrical performance. Precipitation, on the other hand, is not expected to enter the canister since the antenna body and window are effective in this regard. In its

Table I—Measured gain (over isotropic) for 18-GHz antenna without radome

Frequency, (GHz)	Gain, (dBi)	Aperture efficiency, %
17.7	41.5	62.2
18.7	42.1	64.0
19.7	42.4	61.8

customary orientation, the feed is pointing up (see Fig. 2). A variety of feed plug configurations designed to inhibit foreign matter from falling into the feed or accumulating at the opening were fabricated and tested. Each of the plugs considered was formed of commercially-available, expanded, closed-cell, polystyrene with a relative dielectric constant $\epsilon_r \leq 1.03$ and loss tangent 0.002. Each plug was tapered on the outside and inside to inhibit the accumulation of foreign matter and minimize reflected power, respectively. The plugs were cemented in place with an electrically transparent silicone rubber adhesive and then tested for their influence on feed patterns, return loss, and antenna gain across the band. The plug configuration shown in Fig. 9 influenced the feed pattern least, was invisible in return loss and gain measurements, was simplest in design, and was therefore selected.

III. RELATIONSHIP OF FEED TO MIRROR

The topics considered in this and later sections deal primarily with effects which influence the antenna radiation characteristics. It is therefore appropriate to comment briefly on the antenna range facilities for 18-GHz measurements. Pattern and gain measurements are made on a ground reflection range. The source antenna is located close to the ground so that the field illumination across the aperture under test is uniform within one decibel (field uniformity is frequently verified by probing the field in front of the antenna). Use of a pulse transmitter (with a pulse duration of 200 nsec) and gated receiver (which samples the peak amplitude during a 50 nsec interval on the leading edge of the transmitted pulse) assures a measured response free of spurious reflections. The dynamic measurement range at 18 GHz is 70 dB.

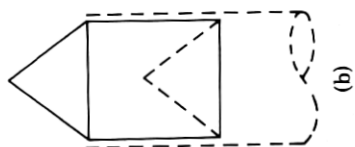
3.1 Axial movement of feed relative to mirror

The canister antenna was designed with the flexibility of allowing feed-paraboloid translation with respect to the mirror. As shown in Figs. 10a and 10b, the feed and paraboloid may be moved in unison (providing, of course, that the feed is always kept at the focal point of the dish) with the electrical aperture of the antenna remaining fixed. Salient antenna dimensions are shown in Fig. 10c.

Moving the feed with respect to the mirror has a pronounced effect upon the antenna radiation pattern. That angular portion of the radiation pattern for which the imaged paraboloid is visible, is influenced more by feed blockage than dish edge illumination (hence the effort to set feed taper for high efficiency). Minimum feed blockage is achieved by selecting a feed with small diameter, and keeping the feed from protruding well above the mirror where it would act as a scattering obstacle. On the other hand, a feed close to the mirror offers the potential for two dele-



(a)



(b)

Fig. 9—Dual mode feed: (a) photograph showing insect seal; (b) diagrammatic depiction of seal.

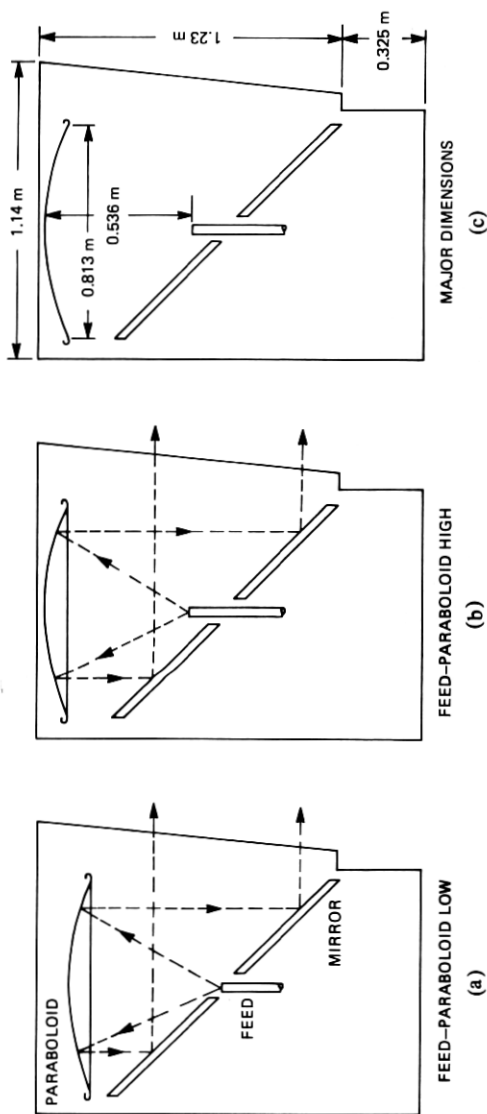


Fig. 10—Schematic depiction of antenna concept: (a) feed-paraboloid in lower-most position; (b) feed-paraboloid elevated; (c) major dimensions.

terious effects. First, a feed too low will allow grazing illumination of the mirror near the hole around the feed, and concomitant pattern degradation. Second, experiments reveal that if the feed directly illuminates the mirror with excessive energy, then the illumination on the dish will be vertically asymmetric in amplitude.⁹ This latter effect would also cause pattern degradation, possibly accompanied by deteriorated cross polarization discrimination.

Optimum feed location was selected by an experimental study of the influence of feed location on antenna radiation patterns. Measurements were made at three frequencies (corresponding to the center and extremities of the 17.7 to 19.7 GHz band) for all polarization states* and differing feed locations. The results, a typical example of which is depicted in Fig. 11 as a smoothed radiation pattern,[†] clearly suggest that a low-profile feed affords the best performance. Therefore, the feed is placed low enough so as not to mask the horizontally directed plane wave, and yet not so low as to allow its spherical wavefront to illuminate the mirror too strongly. At its centerline, the feed axially protrudes above the top surface of the mirror approximately 2.08 centimeters.

3.2 Influence of hole surrounding feed

As shown in Fig. 2, the dual mode feed protrudes up through a hole in the mirror. The mirror itself is constructed of commercially available aluminum plate 0.953 ± 0.013 centimeter thick. The surface is flat within 0.038 centimeter peak over a 1.22-meter span. An aluminum frame is epoxied to the underside to inhibit the plate from sagging under its own weight. The hole in this mirror manifests itself as "feed blockage" and influences the antenna radiation pattern.

A typical set of radiation patterns which exhibit the influence of this hole on radiation suppression is shown in Fig. 12. The three patterns correspond to a mirror with 4.06- and 5.08-centimeter projected diameter holes, and the hole around the feed carefully closed with conducting tape. As these patterns indicate, the presence of the open annulus caused raised sidelobes in the vicinity of 24° to 36° . Data acquired from extensive experimental measurements generally suggests the benefit of making the annulus as small as possible. It is appropriate to add that the annulus cannot be made arbitrarily small since provision must be made for allowing tilt in the mirror. Therefore the hole is designed to have an elliptically shaped projection with a minor diameter no larger than

* Horizontal polarization transmitted—Horizontal polarization received (HH), Horizontal polarization transmitted—Vertical polarization received (HV), Vertical polarization transmitted—Vertical polarization received (VV), and Vertical polarization transmitted—Horizontal polarization received (VH).

[†] Smoothed radiation patterns are prepared by the commonly accepted practice of drawing a smooth line across the peaks in the detailed pattern, thereby forming an envelope of peaks.

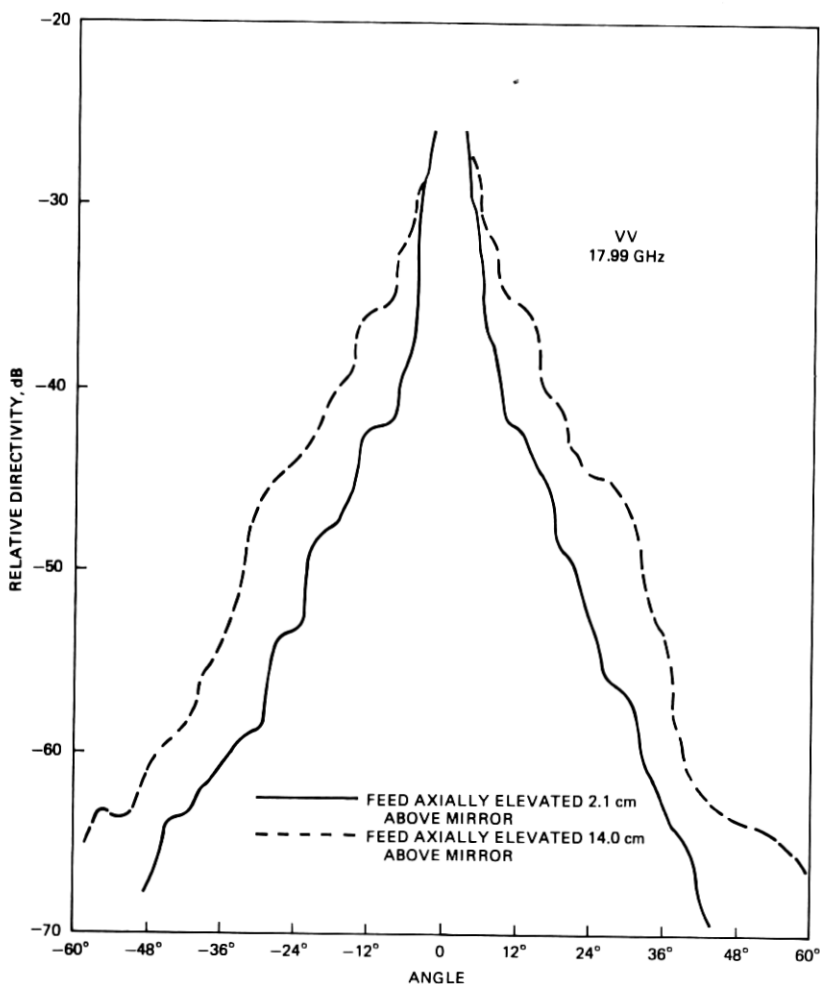


Fig. 11—Influence of feed position relative to mirror on azimuthal radiation pattern envelopes.

necessary for feed placement and orientation, and a major diameter large enough to allow reasonable tilting of the mirror.

IV. MICROWAVE ABSORBER AND ANTENNA RADOME

4.1 Absorber

The inside of the canister antenna is fully lined with microwave absorber. Experimental measurements indicate that absorber is necessary for the suppression of wide-angle sidelobe radiation.

In optimizing antenna performance, a variety of absorbers were con-

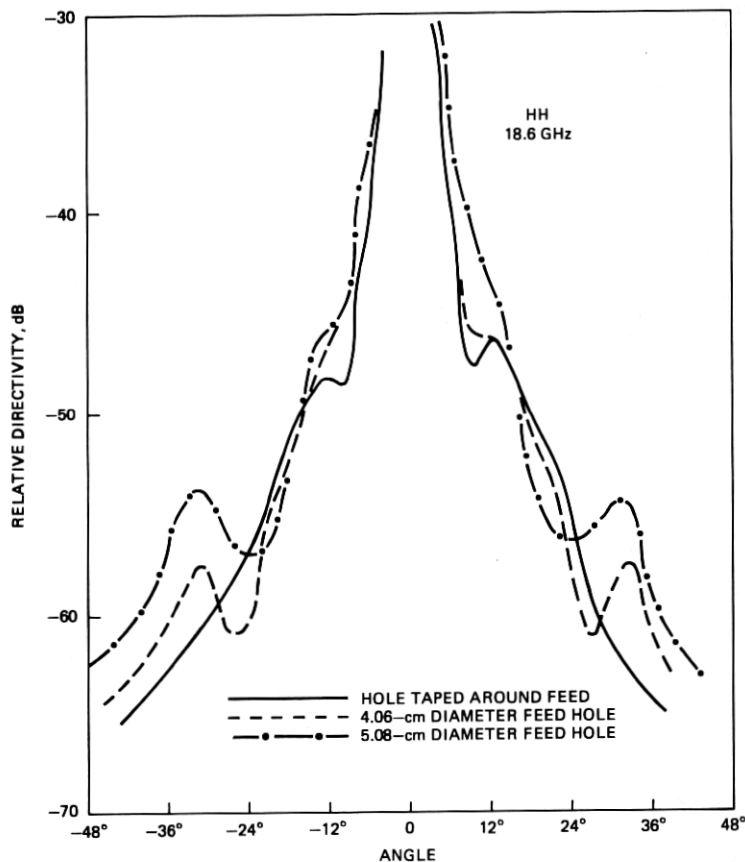


Fig. 12—Influence of feed-mirror annulus on azimuthal radiation pattern envelopes.

sidered, including 1.91-centimeter thick convoluted foam, and 5.08-centimeter thick "hair" absorber. Not only must a suitable absorber provide radiation suppression, but it must be resistant to environmental deterioration. The antenna considered in this paper will provide no absorber protection aside from inhibiting direct exposure to the outdoor elements (sunlight, rain, ice, etc.). Consequently, absorbers for this application should be heat resistant, not inclined to rapid organic decomposition, and impervious to water. Relative to this last point, while the antenna interior will not be exposed directly to rain, it is expected that condensate can form on the inside as the antenna "breathes".

It is useful to list here the respective advantages and disadvantages of the absorbers considered. Since much of the absorber inside the antenna will be subject to grazing incidence of electromagnetic fields rather than normal incidence, the convoluted surface would appear to be de-

sirable since experimentation has confirmed its excellent absorption qualities for varying angles of incidence. In contrast, "hair" has a relatively planar surface and might be expected to yield poorer performance for grazing angles. The convoluted absorber is made of an open-cell foam material while the "hair" is an open mat. Normally the "hair" absorber would have no tendency to hold water, while the convoluted foam could pick up water in a manner analogous to a sponge. To remedy this effect, the foam was covered with a sprayed Hypalon* coating approximately 0.076 millimeters thick. Hypalon in itself is an excellent coating because of its electromagnetic transparency and proven resistance to weathering. However, the coating was easily perforated by fingers during installation. Finally, "hair" was significantly less expensive than the convoluted material, or even flat foam absorbers of comparable thickness.

As a first step in assessing absorber performance, radiation patterns were made with no absorber, partial absorber, and a complete absorber lining of the antenna interior. The resulting radiation patterns using "hair" absorber are depicted in Fig. 13a. As this figure indicates, the addition of absorber dramatically reduces the wide-angle radiation of the antenna. The next step in the evaluation was to run separate patterns with the convoluted and hair absorber at three frequencies within the band for a variety of linear polarizations. The results, an example of which is shown in Fig. 13b, suggest that convoluted absorber generally affords slightly better performance. However, the differences are minor and because of the cost and weatherability advantages of the "hair," it is preferred in this application.

4.2 Radome

Radomes have been traditionally used on high performance line-of-sight antennas used in the 4-, 6-, and 11-GHz common carrier bands. These radomes are called "thin" because the 0.762- to 1.016-millimeter fiber glass membranes are only $\lambda/30$ thick at the highest frequency. At frequencies near 20 GHz, preliminary tests on the canister antenna indicate that from a pattern standpoint, a satisfactory thin radome would have to be less than approximately 0.305 millimeters in thickness. Such a thin radome would prove structurally inadequate. For that reason, attention was focused on half-wavelength radomes.

A radome used in the tests to be described was a solid laminate constructed of epoxy resin and a low-loss fiber glass called E-glass. The dielectric constant of the laminate was thought to be 4.0 so the radome was made 0.399 centimeters thick for electrical tuning at 18.7 GHz. Subsequent measurements indicated that the radome was actually tuned at approximately 18.3 GHz, inferring a dielectric constant of 4.3 (this latter

* Registered trademark of E. I. duPont de Nemours & Co., Inc.

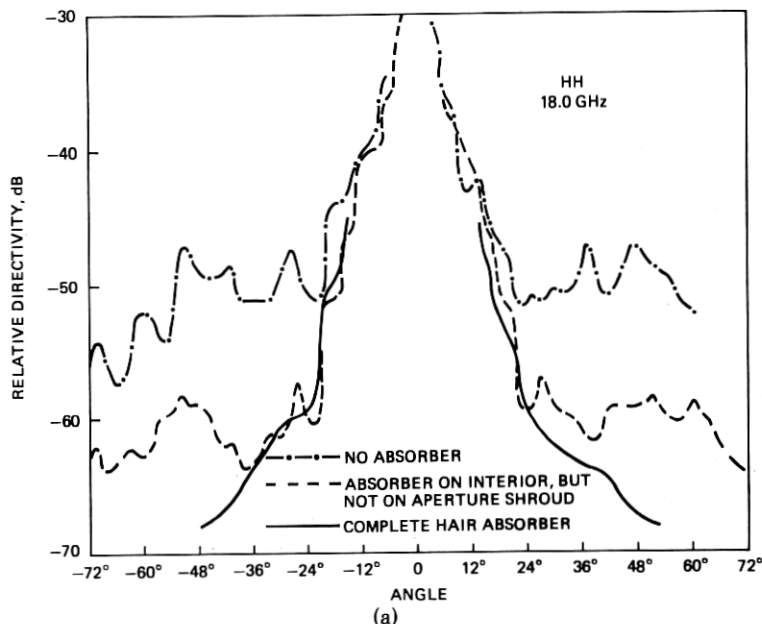


Fig. 13—Influence of microwave absorber on azimuthal radiation pattern envelopes: (a) presence or lack of absorber; (b) type of absorber.

value is in accord with the commonly accepted value for this composite material). The loss tangent is 0.016.

Figures 14a and b depict representative results obtained with and without the radome on the antenna. Figure 14a indicates that measurements made near the tuned point show the radome to have little influence on the antenna radiation patterns. This is also true of the cross polarized response. Figure 14b presents measured results near the edge of the band. For this case the radome does perturb the principal polarization wide-angle radiation characteristics, though the sidelobe suppression still meets the design objectives. The common explanation of this effect is that energy is reflected back into the antenna and subsequently reradiated. Indeed, measurements made on this radome indicate that specularly reflected power is 35 dB down at 18.3 GHz, but only 13 dB to 14 dB down at 19.7 GHz.

V. MIRROR TILT AND FEED POSITION SENSITIVITY

5.1 Mirror tilt

Pairs of antennas used for point-to-point transmission are carefully oriented in elevation and azimuth to electrically point exactly at each other. For the canister antenna with relatively narrow beam width (3

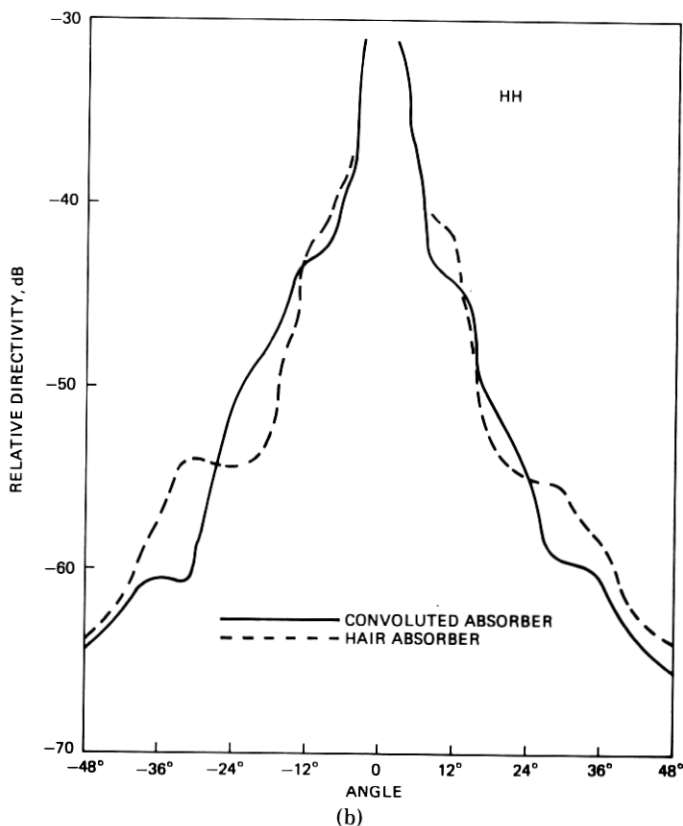


Fig. 13—(continued)

dB beam width of 1.33°), this orientation is performed by peaking the received signal while adjusting the azimuthal and elevation angle. The azimuthal orientation is accomplished by rotating the entire antenna in its supporting cross-arm (see Fig. 1). The elevation angle is adjusted by rotating the mirror about the horizontal axis so as to tilt the beam up or down. It is readily shown that as the mirror is tilted through the angle θ_m , the beam moves $\theta_b = 2\theta_m$. The overall influence of reflector tilt on gain and pattern is covered in this section.

Reference radiation patterns were first measured with the mirror in the "nominal" 45° position (beam horizontal). Patterns were then measured with the mirror in a "tilt up" and "tilt down" position of approximately $\theta_m = \pm 1.5^\circ$. In both cases the entire antenna was tilted 3.0° in the opposite direction to compensate for the beam tilt. This is done to maintain bore-sight beam orientation between the source and antenna. These measurements then establish the effect of the internal interaction of the plane reflector with other antenna parts. It should also

be noted that by tilting the antenna canister to compensate for reflector tilt, the patterns so obtained do not quite lie in the azimuthal plane, though the difference is slight.

As expected, it was observed that tilting the mirror causes a decrease in received signal level, but this signal is completely restored by compensatory antenna tilt. Therefore, gain changes do not occur with modest

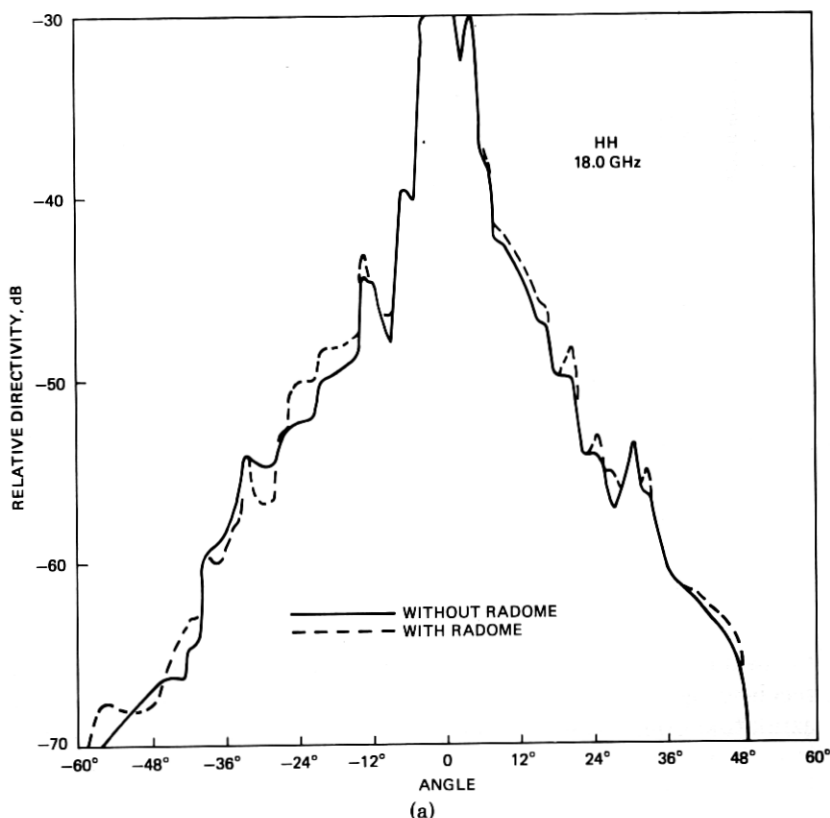


Fig. 14—Influence of half-wavelength solid laminate radome on azimuthal radiation patterns: (a) 18.0 GHz; (b) 19.7 GHz.

beam tilt. The tilt experiments were done with and without a radome on the antenna, and for both polarization states of the antenna. Tilting the mirror is found to have almost no influence on the antenna sidelobe response. At most, 3 or 4 dB changes are noted at -55 dB levels near 30° . These small changes in sidelobe level are felt to be of little consequence because they are so far down from the main beam and do not change the angle at which the patterns drop beneath -60 dB.

5.2 Feed position sensitivity

Feeds with diameters commensurate to a wavelength have phase centers located approximately in the plane of their aperture. Therefore the dual mode feed used in this antenna is positioned to have its aperture coincident with the focal point of the paraboloidal reflector. Nevertheless, it is of interest to determine the sensitivity of feed position to deg-

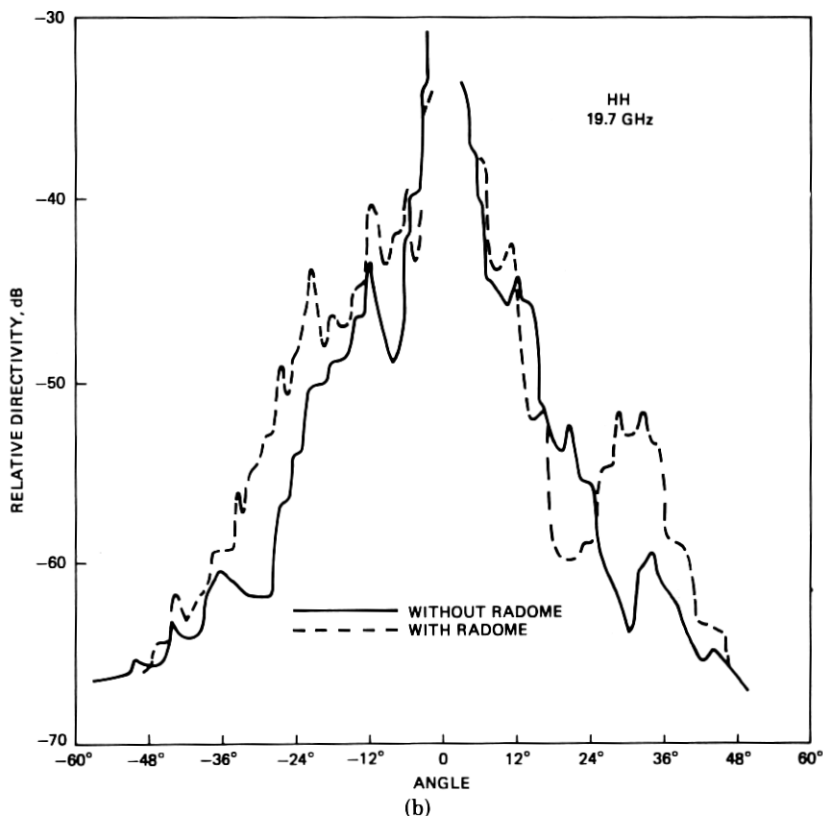


Fig. 14—(continued)

radation in antenna performance. Three conditions were examined: feed skew (feed axis inclined to paraboloidal axis of symmetry), feed linear displacement (feed and paraboloidal axis parallel, but feed axially or laterally displaced), and feed-polarizer twist. Briefly the tests show that up to 1° of feed skew, axial movement of up to 0.25 centimeter, and lateral displacement of up to 0.25 centimeter have little or no discernible influence. Feed-polarizer twist of up to 3° has no effect on gain, a minimal effect on pattern (first sidelobe increased 1 dB), but as expected, does deteriorate cross polarization discrimination.

These tests indicate that antenna performance is not overly sensitive to feed position, and allow for rather lenient support bracket tolerances which are easily maintained at minimal expense.

VI. ANTENNA RETURN LOSS

Transmitted power which is reflected back to the feed manifests itself as antenna return loss. The sources of reflected power in this antenna are: (i) feed mismatch including insect seal, (ii) parabolic dish, and (iii) radome. These items are individually treated below.

Since the dual mode feed has a circular cross section and the polarization diplexer which will be used with this antenna was designed in square waveguide, a suitable transition was designed to connect the two. Such a transition requires the conversion of two dominant, orthogonal, TE_{10}^o modes in WS-42 to two dominant, orthogonal, TE_{11}^o modes in WC-50. For this purpose, a four-inch linear tapered transition with no measurable transmission loss and a return loss of better than 40 dB (reflection coefficient <0.01) was electroformed. Swept frequency return loss measurements on the feed with insect seal and linear transition were made, and are depicted in Fig. 15a. The return loss across the entire frequency range is better than 29 dB, corresponding to a VSWR ≤ 1.075 or reflection coefficient ≤ 0.035 .

Return loss of the complete antenna was measured across the band of interest. Figure 15b shows this performance as a solid line for the antenna radiating into free space. The poorest return loss within the band is approximately 23 dB. A simple vector separation analysis, based on the assumption that the only contributions to the total returned power are the feed and paraboloid with radome, produced the dashed line as the contribution of the paraboloid and radome alone. Measurements indicate that with the mirror in its normal position, the contribution of the radome to total return loss is negligible since energy reflected back into the canister by the radome is not focused at the feed. This is still true with the antenna beam tilted down 3° since the reflected energy from the radome is 3° off boresight.

The resulting dish contribution of approximately 28 dB agrees well with a computed value of 26.8 dB obtained from the equation

$$\text{Return loss} = 20 \log \frac{4\pi f}{\lambda G_f} \quad (7)$$

In this equation, f is the focal length of the paraboloid (0.536 meters), and G_f is the feed gain. Feed gain has been computed as 12.9 dB at 18.7 GHz by direct integration of the normalized feed radiation pattern. The equation above is derived by determining what fraction of power radiated by the feed, W_f , is recaptured by the feed. The power density in the axial

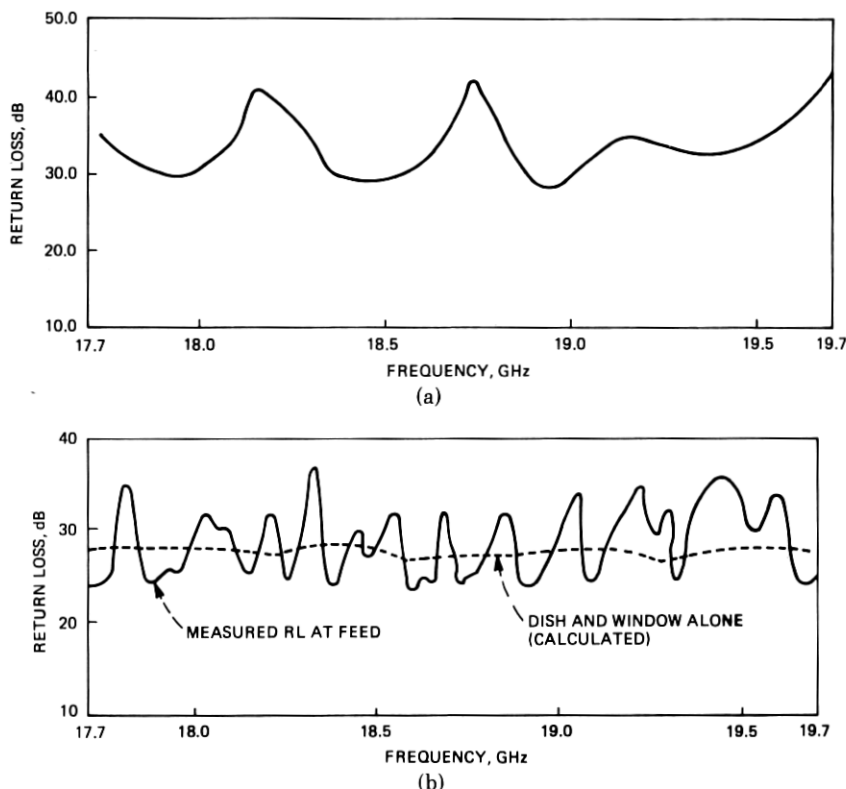


Fig. 15—Return loss performance: (a) dual mode feed alone; (b) return loss with feed in canister antenna.

region of the dish is $P_d = W_f G_f / 4\pi f^2$. This power density is reflected back toward the feed as a plane wave and captured with effective area $A_{\text{eff}} = \lambda^2 G_f / 4\pi$. The power captured by the feed, W_c , is $W_c = A_{\text{eff}} P_d = W_f (\lambda G_f / 4\pi f)^2$, and eq. (7) follows directly.

VII. CONCLUSION AND SUMMARY OF ANTENNA CHARACTERISTICS

The design and experimental optimization of a canister antenna are reviewed in this paper. The influence of antenna feed, parabolic reflector, radome, absorber and mirror on gain, radiation pattern, and return loss is considered.

The measured gain of the antenna, virtually independent of polarization, is stated in Table I. These values of gain, measured without a radome in place, correspond to an approximate aperture efficiency of 62 percent. The loss of the solid, half-wavelength-thick radome is 0.4 dB.

The principal and cross polarized response of the antenna is illustrated

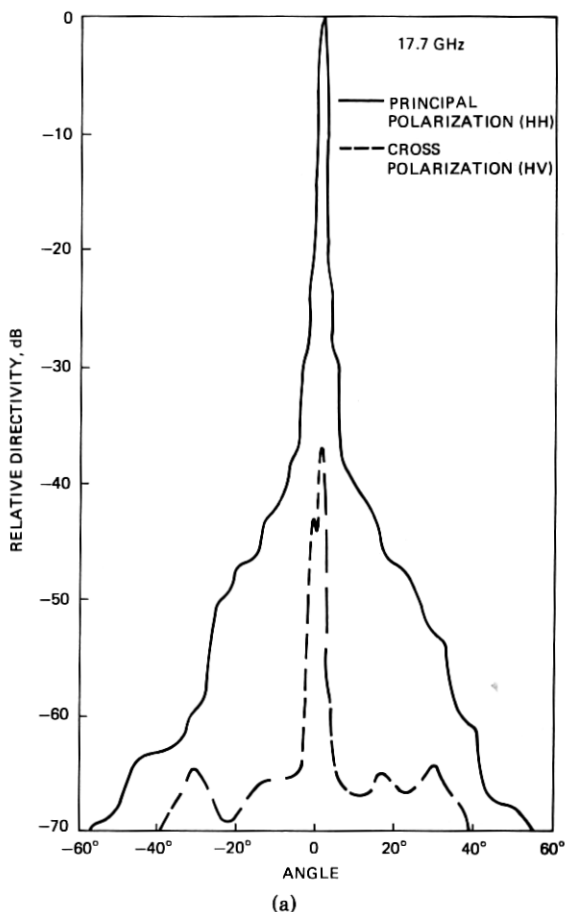


Fig. 16—Principal (HH) and cross polarized (HV) smoothed azimuthal radiation pattern envelopes measured with radome installed: (a) 17.7 GHz; (b) 18.7 GHz; (c) 19.7 GHz.

by the smoothed radiation patterns presented in Fig. 16. This figure presents the 17.7 GHz, 18.7 GHz and 19.7 GHz horizontally polarized response (HH) and the vertically polarized antenna response to a horizontally polarized transmitted signal (HV) with the half-wavelength radome on the antenna. Similar radiation patterns are obtained for the VV and VH polarizations. This is to be expected since the antenna design is essentially polarization independent provided the dual mode feed affords a balanced E and H plane illumination of the paraboloid. As noted earlier, such a balanced illumination is reasonably achieved. The principal polarization patterns include perturbation introduced by the radome. A comparison of these patterns with corresponding patterns measured without a radome reveals that sidelobe levels beneath -40 dB

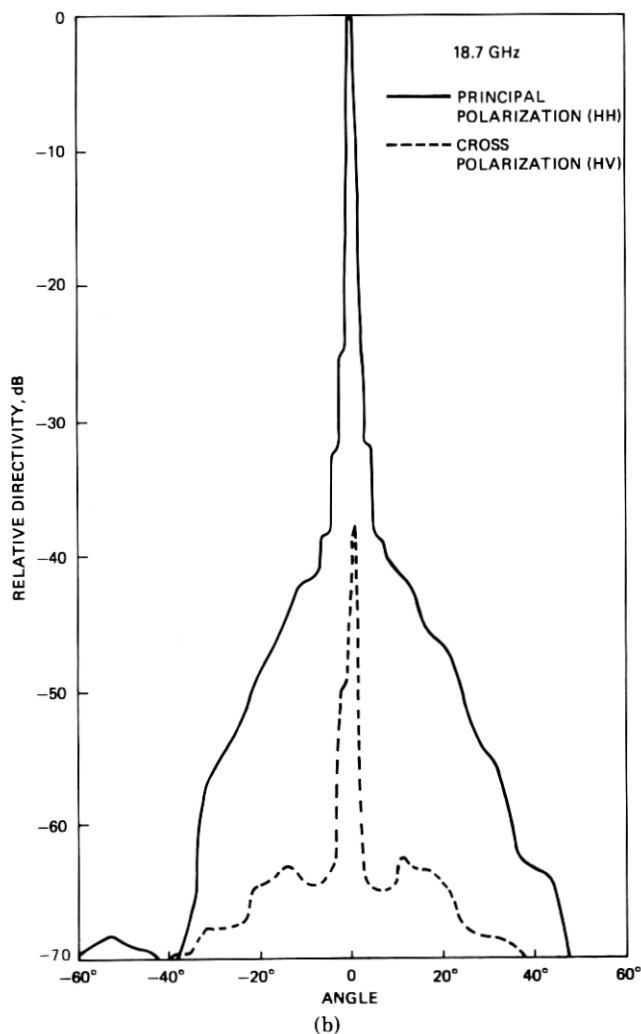
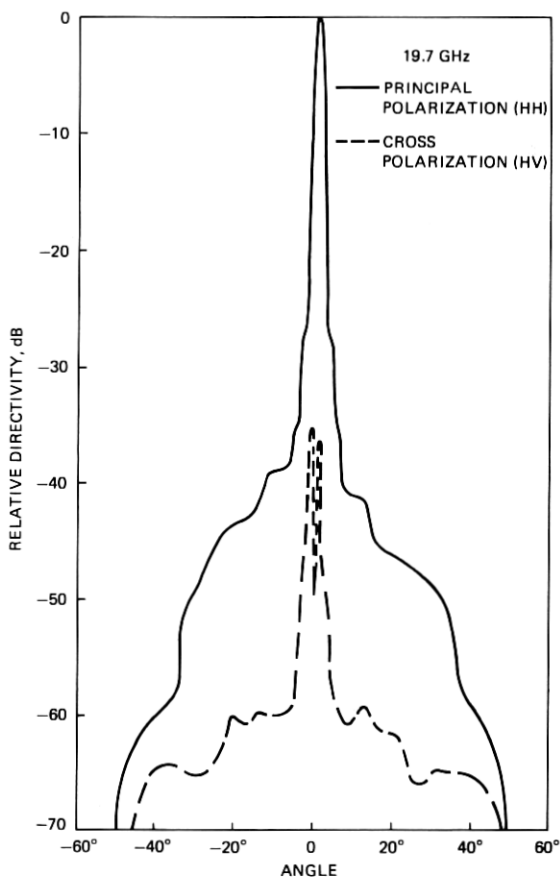


Fig. 16—(continued)

are primarily affected, with the largest pattern deterioration occurring at the lowest radiation levels, and being most pronounced the further the frequency departs from 18.3 GHz (the "tuned" frequency for this radome). From Fig. 16, we also note that the on-axis cross polarization discrimination is in the mid to upper 30 dB range, confirming an estimate offered in an earlier paper dealing with this antenna concept.⁴ The influence of mirror tilt and feed positioning is also assessed. It is shown that modest amounts of mirror tilt (e.g., $\pm 1.5^\circ$) and inaccurate feed positioning have minimal effect upon the antenna pattern and gain.



(c)

Fig. 16—(continued)

Return loss measurements have been made on the complete antenna and individual components. The major contributors to reflected power are feed mismatch and the parabolic dish. The worst-case return loss of the feed with transition is approximately 29 dB. The return loss of the paraboloid is estimated to be 28 dB. With the mirror in its nominal position, the radome contribution is negligible. The poorest total return loss measured (which occurs at a different frequency than the worst-case feed contribution) within the band is approximately 23 dB.

As mentioned earlier, the antenna described in this paper was designed for an 18 GHz digital radio system. The particular antenna described herein was specifically designed to afford certain degrees of flexibility which would not be required after identification of those parameters which influence antenna performance. For example, the canister was

oversized to permit installation of a variety of absorbing materials and so the paraboloid could be translated up and down relative to the mirror. With completion of the performance characterization, certain changes were made in the final antenna design. The final design will allow beam pointing of $\pm 8^\circ$. To accomplish this and assure adequate return loss, the radome will be fastened to the antenna in such a manner that the beam will not point within 1.5° of the normal to the radome surface. Perhaps the most significant change to be implemented in the final design is a larger paraboloidal reflector with a 0.864-meter diameter. This reflector (which necessitates a somewhat larger mirror) will afford approximately 0.5 dB more gain. This increased gain is just slightly more than the 0.4 dB loss introduced by the radome. It is expected that the antenna with a 0.864 meter dish will have a radiation pattern quite similar to that measured on the developmental model, and a total return loss of approximately 23 dB.

VIII. ACKNOWLEDGMENT

The authors are pleased to acknowledge the following Bell Laboratories colleagues and their contributions: A. B. Crawford and R. H. Turrin for their initial studies and subsequent insights into aspects of the antenna performance; I. Anderson for his work in experimental and analytical interpretation of the antenna radiation; N. R. Lampert for various aspects of the physical design of the antenna; and C. P. Bates for helpful discussions and general guidance of the activities.

REFERENCES

1. C. A. Siller, Jr., and P. E. Butzien, "A Radio Relay Antenna for Application at 18 GHz," 1974 IEEE/AP-S Symposium Program and Digest, Atlanta, Georgia, June 10-12, 1974, pp. 253-255.
2. A. C. Longton, "DR 18—A High Speed QPSK System at 18 GHz," 1976 International Conference on Communications, Conference Record, II, Philadelphia, June 14-16, 1976, pp. 18-14 to 18-17.
3. J. J. Kenny, "18-GHz Channelization for 275 Mb/s Transmission," Paper presented at URSI meeting, Boulder, Colorado, August 22, 1973.
4. A. B. Crawford and R. H. Turrin, "A Packaged Antenna for Short-Hop Microwave Radio Systems," *B.S.T.J.*, 48, No. 6 (July-August 1969), pp. 1605-1622.
5. T. S. Chu, "Maximum Power Transmission Between Two Reflector Antennas in the Fresnel Zone," *B.S.T.J.*, 50, No. 4, April 1971, pp. 1407-1420.
6. D. Herbison-Evans, "Optimum Paraboloid Aerial Design," Report No. 66012, Signals Research and Development Establishment, Ministry of Aviation, Christchurch, Hants, September 1966.
7. I. Anderson, unpublished memoranda.
8. R. H. Turrin, "Dual Mode Small Aperture Antennas," *IEEE Trans. Ant. Prop. (Communication)*, AP-15, No. 2, March 1967, pp. 307-308.
9. R. H. Turrin, personal communication.

